

Evidence of vortex kink formation in antidotted layered superconductors

A. Angrisani Armenio, C. Attanasio, L. V. Mercaldo, S. L. Prischepa,* M. Salvato, and L. Maritato[†]
Dipartimento di Fisica "E.R. Caianiello" and INFM, Università degli Studi di Salerno, 84081 Baronissi (Sa), Italy

V. N. Kushnir

State University of Informatics and RadioElectronics, P. Brovka Str. 6, 220013 Minsk, Belarus

S. Barbanera

IESS-CNR, Via Cineto Romano 42, Roma, I-00146, Italy

(Received 17 December 2001; published 28 May 2002)

The angular dependence of the critical current density J_c in external magnetic field has been measured in Nb/CuMn multilayers with and without a regular array of antidots. The multilayers without antidots behave coherently to what has already been reported in the literature, showing, for sufficiently high anisotropy, dissipation related only to the magnetic-field component perpendicular to the layers, H_\perp . This behavior is generally explained in terms of the presence of kinked vortices. The kink formation has been directly detected in the antidotted samples, where low angle modulation of J_c , related to single vortex kinks entering the system, has been found. The presence of kinks explains also the unusual scaling of J_c vs H_\perp found at low anisotropy in the antidotted case up to a value of the angle related to the geometrical structure of the system.

DOI: 10.1103/PhysRevB.65.212503

PACS number(s): 74.60.Ge, 74.60.Jg, 74.80.Dm

After the discovery of high-temperature superconductors (HTS's) the study of the vortex dynamics in superconducting layered systems has gained large interest because of the many intriguing vortex related phenomena predicted and observed in these materials.¹⁻³ As an example, in the presence of strong anisotropy, the elasticity and the flexibility of the vortex lattice can change dramatically,¹ affecting temperature and angular dependence of the upper critical field H_{c2} and of the critical current I_c .⁴⁻¹⁰

In tilted external magnetic fields, layered superconducting systems may present, under suitable conditions, vortex kinks.¹¹⁻¹⁴ Although many effects have been ascribed to the presence of such kinks,^{1,6,15,16} a direct observation of their formation is still lacking. Artificial layered structures are particularly suited to this purpose. Different parameters can be adjusted in a controlled way and the consequences on the superconducting properties can be observed in various regimes. Moreover, in conventional superconductor based multilayers the use of lithographic techniques to design suitable geometries is more simple and effective when compared to HTS based systems. As a matter of fact, dotted and antidotted thin-film nanostructures based on conventional superconductors have been investigated in the last years revealing many interesting phenomena.¹⁷⁻¹⁹

In this paper we report on measurements of the angular and magnetic-field dependence of the critical current density J_c in superconductor (Nb)/spin-glass (CuMn) multilayers with and without a regular array of antidots for different anisotropy values γ . Magnetic spacers, when compared to metallic spacers, decouple the superconducting layers at smaller thicknesses, forcing the superconducting order parameter of the system to modulate over distances closer to those observed for HTS's. Moreover, the use of a spin-glass alloy like CuMn as spacer opens up the possibility to easily obtain a large range of anisotropy values by changing the Mn percentage or the Nb and CuMn relative thicknesses.^{4,20-22}

By comparing the superconducting behaviors in the samples with and without antidots and with different anisotropy values, we point out the influence of the antidot array on the vortex properties. Multilayers without antidots behave coherently to what has already been reported in the literature.¹⁰ For the samples with antidots, J_c depends only on the perpendicular component H_\perp of the applied field H_a up to a certain value of the angle θ between the field and the plane of the sample, related to the sample thickness and the distance between neighboring antidots. This behavior is attributed to the presence of kinked vortices, directly revealed by the low angle steplike dependence found for J_c vs θ , which can be seen as a signature of single kinks successively entering the system.

The multilayers were grown by dc sputtering on Si(100) substrates,²⁰ starting with CuMn and ending with Nb. The samples without antidots were patterned by chemical etching into 50- μm -wide and 1-mm-long stripes. The other samples present a square array of antidots regularly distributed over a $200 \times 200\text{-}\mu\text{m}^2$ area. The diameter of the antidots is $d = 0.5\ \mu\text{m}$ and the lattice distance is $D = 1\ \mu\text{m}$. The details about the preparation of these samples, obtained by lift-off procedure after an electron-beam lithography, are reported elsewhere.²¹

All the samples present a well defined layered structure, as shown by low angle x-ray diffraction.²² The multilayers have been characterized by measuring the upper critical fields, extracted at the midpoint of the resistive transitions $R(T,H)$, both in perpendicular and parallel direction with respect to the layers. From these measurements the anisotropy of the samples, $\gamma = \xi_\parallel / \xi_\perp$, has been extracted.²³ Here ξ_\parallel and ξ_\perp are, respectively, the in-plane and out-of-plane coherence lengths at zero temperature. Relevant parameters of the samples discussed in this paper (A1, A2 without antidots; B with antidots) are reported in Table I.

TABLE I. Relevant sample parameters: layer thicknesses, Mn percentage, critical temperature, zero-temperature in-plane and out-of-plane coherence lengths, anisotropy parameter, characteristic angles.

Sample	d_{Nb} (Å)	d_{CuMn} (Å)	% Mn	T_c (K)	ξ_{\parallel} (Å)	ξ_{\perp} (Å)	γ	θ_{2D} (deg)	θ_{3D} (deg)
A1	250	45	2.7	4.7	104	21	5.0	11	59
A2	250	17	2.7	4.8	64	53	1.2	40	68
B	250	28	2.0	6.5	97	54	1.8	29	60

The critical current was measured using a dc voltage criterion of $5 \mu\text{V}$. For the samples with antidots the corresponding current density was calculated using as available area for current flow the value obtained by subtracting the antidot contribution from the total cross section of the sample. The magnetic field was always applied perpendicular to the average current direction [see inset of Fig. 1(a)], and the angle θ was varied from -90° to 90° with an accuracy of $\pm 0.1^\circ$. In our configuration $\theta=0^\circ$ corresponds to parallel orientation of the field. The measurements were made for all the samples at a comparable value of the reduced temperature, namely $t=T/T_c \approx 0.65$, with T_c the superconducting critical temperature of the multilayers. The temperature stabilization during the measurements was ± 0.01 K.

In Fig. 1(a) the critical current density for sample A1,

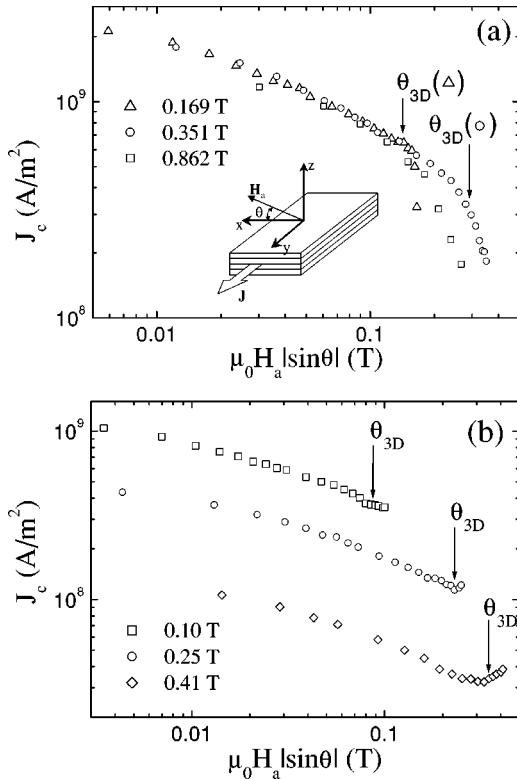


FIG. 1. J_c versus H_{\perp} at different applied field values for sample A1 at $T=3.10$ K (a) and sample A2 at $T=3.18$ K (b). Arrows indicate the θ_{3D} values. The applied field values are reported in the legends. Inset of (a): Schematic of magnetic field \mathbf{H}_a and transport current \mathbf{J} orientation during the measurements.

without antidots and with $\gamma=5$, is plotted as a function of the perpendicular component of the applied magnetic field $H_{\perp}=H_a|\sin\theta|$, obtained by keeping fixed the magnitude of the external applied field H_a and varying the value of the angle θ . The data have been acquired at $T=3.10$ K for three different values of the magnetic field H_a up to $\mu_0 H_a = 0.862$ T. All the curves scale on a single one, indicating that J_c is regulated only by H_{\perp} , until high angles ($\approx 60^\circ$) are approached.²⁴ No scaling of J_c vs H_{\perp} is observed for lower anisotropies, as shown in Fig. 1(b) for sample A2, without antidots and with $\gamma=1.2$, for three different fields (0.1, 0.25, and 0.41 T) at temperature $T=3.18$ K. In this case the curves do not collapse onto a single one. Nb/CuMn multilayers without antidots and with $\gamma \leq 3$ have shown similar behaviors, in agreement with the experimental results observed in other artificial multilayered systems and explained invoking the influence of anisotropy on the vortex topology.¹⁰

When dealing with a layered system in tilted external magnetic fields, the tilting angle θ determines the vortex structure.^{14,25} For small values of the applied fields a single vortex approach is valid. At $\theta > \theta_{3D}$, with $\tan[(\pi/2) - \theta_{3D}] = \xi_{\parallel}(T)/\Lambda$ and Λ the structural modulation period, the vortices are well described as three-dimensional (3D) objects in an anisotropic superconducting medium. For $\theta < \theta_{2D}$, with $\tan[(\pi/2) - \theta_{2D}] = \gamma$, the vortices have a two-dimensional (2D) character and are coupled by Josephson-like vortices through adjacent layers. When $\theta_{2D} < \theta < \theta_{3D}$, vortex lines can be considered as a set of 2D vortices with 3D coupling among them. Moreover, for strongly anisotropic systems in an external magnetic field exactly parallel to the layers ($\theta=0$), the layered structure itself works as an array of intrinsic pinning centers, allowing the vortex cores to fit in between the superconducting planes. When θ is increased, the vortex lattice remains locked, with flux trapped parallel to the layers, until a critical angle θ_c is reached.¹³ This critical angle, given by $\sin\theta_c = 4\pi\epsilon_K/\phi_0 H_a$, is related to kink formation in the flux lines. Here ϕ_0 is the flux quantum, and ϵ_K is the anisotropy-dependent energy per unit length of the flux line in the perpendicular direction.

The type of coupling present between superconducting layers in the case of our Nb/CuMn multilayers is not exactly known. The concept of kinked vortices is generally related to the topology of the flux lines and in the literature the scaling behavior of the J_c vs H_{\perp} curves for different layered systems with high anisotropy is interpreted in terms of the presence of kinked vortices moving within the superconducting planes.^{10,16} If we apply a similar interpretation for sample A1, the presence of scaling for $\theta < \theta_{3D} \approx 59^\circ$ [Fig. 1(a)], implies that, assuming valid the general description in Refs. 13, 14, and 25, θ_c is at least equal to θ_{\min} , the smallest measured angle ($\theta_c \leq \theta_{\min} \approx 1^\circ$). On the other hand, the lack of scaling for sample A2 [Fig. 1(b)] indicates that kinks are not playing a strong role in the vortex dynamics, as it should be when the value of θ_c is larger than $\theta_{3D} \approx 68^\circ$, the angle beyond which the concept of kinks starts to be not valid anymore. The expected dependence of ϵ_K on the anisotropy is $\epsilon_K \sim 1/\gamma^2$, if ϵ_K is related to the superconducting condensation energy.¹

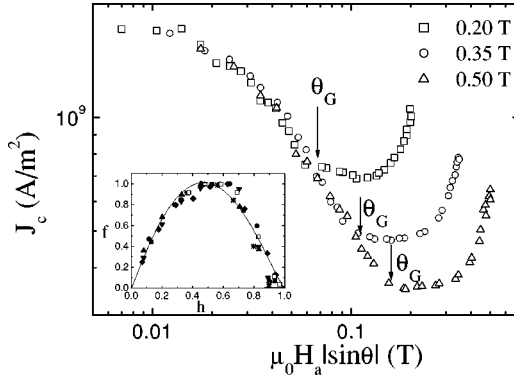


FIG. 2. J_c versus H_{\perp} for sample B at $T=4.2$ K at different applied field values. Arrows indicate the θ_G values. Inset: Reduced pinning force f versus reduced perpendicular field h for sample B at seven different temperatures in the range 1.9–4.2 K. Solid line is the $f=h(1-h)$ law.

Therefore a value of the ratio between the energies for the two samples $\epsilon_K(A2)/\epsilon_K(A1) \approx \gamma^2(A1)/\gamma^2(A2) \approx 17$ is expected. In fact, a value of the same order is found when estimating the energy ratio by using the two limiting values found for θ_c . This observation can be taken as another indirect proof of the presence of kinked vortices in sample A1.

The high angle behavior of the curves in Figs. 1(a) and (b) also supports the idea of the presence of kinks in A1. For sample A2 an upturn in J_c is observed when $\theta = \theta_{3D} \approx 68^\circ$, which can be related to the presence of extended pinning centers in the direction perpendicular to the layers, as it should be in the case of edge pinning¹⁰ or grain-boundary pinning (for example, due to the thin-film columnar growth²⁶). This upturn is not observed in the curves of Fig. 1(a), where J_c drops suddenly when $\theta = \theta_{3D}$. The lower pinning efficiency of the extended defects in sample A1 can be interpreted again in terms of the different topology of the flux lines in very anisotropic systems. Even in the angular region where 3D behavior is expected, they are made of strongly interacting 2D vortices and thus can move more easily when compared to rigid 3D vortices.

Antidotted samples show different behavior. The typical dependence of J_c vs H_{\perp} for antidotted systems is plotted in Fig. 2 for sample B at $T=4.21$ K for three different fields. The anisotropy parameter of the sample is $\gamma=1.8$, a value at which no scaling of J_c vs H_{\perp} is observed in the absence of antidots. In this case, scaling is found up to a value of the angle $\theta_G < \theta_{3D} \approx 60^\circ$ and, for all the curves in Fig. 2, we have $\theta_G \approx 18^\circ$, independently from the value of the applied magnetic field. Beyond θ_G , the curves do not scale and present a sudden upturn when θ_{3D} is approached, as in the case of the samples without antidots and with comparable anisotropy. Moreover, if we replot the data at $\mu_0 H_a = 0.2$ T of Fig. 2 as J_c vs θ , clear J_c steps are present at small angles with angular intervals of $\Delta\theta \approx 3^\circ$ (Fig. 3). In between the current falls, the curve is more or less flat, showing almost constant J_c values. This $J_c(\theta)$ modulation is observed only in the limit of low external magnetic field H_a .

In the data analysis, on the basis of the observed pinning force dependence on the external magnetic field, we can rule

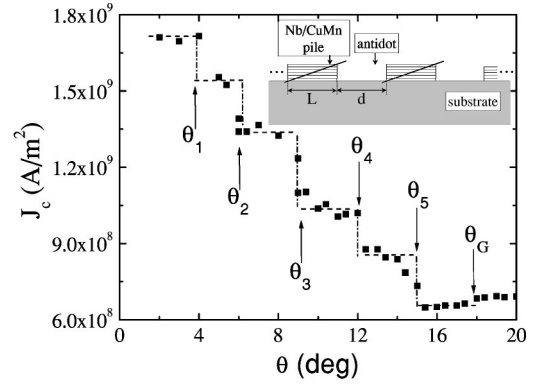


FIG. 3. Angular dependence of J_c at low angles at $T=4.2$ K and $\mu_0 H_a = 0.2$ T for sample B. Dashed line is a guide to the eye. Inset: Schematic of a vertical section of sample B, where piles of Nb/CuMn multilayer are intercalated with empty regions (antidots). The lines indicate the direction of the magnetic field at the orientation $\theta = \theta_G$, while the bias current flows perpendicular to the plane of the figure.

out the presence of edge pinning. In the inset of Fig. 2, we show the behavior of the reduced pinning force $f = F_p/F_{pmax}$, measured at $\theta = \pi/2$, versus the reduced magnetic field $h = H_a/H_{c2\perp}$ for sample B in the temperature range 1.9–4.2 K. All the data scale on a single curve which is well fitted to the $h(1-h)$ law, implying a single vortex pinning mechanism.²⁷ In the case of edge pinning the expected scaling law is $h^{0.5}(1-h)^2$ with a maximum of the pinning force at $h \approx 0.2$.²⁸ As a matter of fact the introduction of antidots, with a very small value of the matching field (~ 20 Oe) and with $d \gg \xi_{\parallel}, \xi_{\perp}$, does not improve the pinning forces. Actually it locally reduces the pinning strength in the narrower zones between adjacent antidots (piles in the inset of Fig. 3), where the bias current density is higher.²¹

The scaling of the curves in Fig. 2 at $\theta < \theta_G$ is somehow surprising in terms of the analysis performed on the samples without antidots. The anisotropy of sample B implies a critical angle $\theta_c > \theta_{3D} > \theta_G$, while scaling is observed in Fig. 2, starting from the lowest measured angles. This result suggests that the presence of antidots enhances the role played by the kinks. With antidots, a large number of superconductor-air interfaces is introduced where, due to the wall roughness, the formation of perpendicular segments of flux lines is favored.⁵ In this picture the absence of J_c vs H_{\perp} scaling at angles $\theta > \theta_G$ is easily understood, considering that $\theta_G \approx 18^\circ$ is very close to the angle defined as $\tan^{-1}(t/L) = 18.4^\circ$, where $t \approx 1670$ Å is the sample thickness and $L = 5000$ Å is the distance between the edges of neighboring antidots (see inset of Fig. 3). In fact, at angles larger than θ_G a relevant fraction of vortices does not cross the antidot interfaces, kink formation is not favored, and the vortex dynamics is that expected in the case of an ordinary layered system with small anisotropy.

Finally, the presence of kinks in sample B at $\theta < \theta_G$ is directly confirmed by the steps in the angular dependence of J_c at low angles (Fig. 3), where the measured interval $\Delta\theta \approx 3^\circ$ is very close to the geometrical angle given by $\tan^{-1}(L/L) = 3.2^\circ$. In a single vortex approach, valid in the

low-field regime where the $J_c(\theta)$ modulation is observed, the interpretation of these data in terms of kinks entering the system is straightforward. At $\theta = \theta_i$, with $i = 1, \dots, 5$ (see Fig. 3), perpendicular flux lines are created, with length of the order of Λ , joining parallel segments of vortices pinned by adjacent nonsuperconducting layers. These perpendicular flux lines can move inside the superconducting layers producing the observed J_c drops. Therefore this J_c versus θ steplike behavior gives an important indication about the topology of the vortex kinks in the system, even though further experimental work is needed to point out the influence of the Nb and CuMn single thickness on the nature of the flux lines. The slight disagreement found among the $(\theta_{i+1} - \theta_i)$ values might be related to small differences in the layer thicknesses of the nominally periodic structure. We want to stress that the steplike J_c dependence is observed only below θ_G where the formation of kinks is favored.

In principle this modulation could be also present in layered samples without antidots, but would be limited to a very small angular interval, close to $\theta = 0$. In that case, in fact, $\Delta\theta$ would approximately be $\tan^{-1}(\Lambda/w)$, where w is the width of the sample, which can be several orders of magnitude larger than Λ . Similar limitation on the angular range is expected for HTS's, due to the very small period of the order-parameter modulation in these structures. The presence of a regular array of antidots is therefore essential to allow the observation of the J_c steps in an accessible angular interval.

Moreover, the presence of the antidot array plays a crucial role in making the height of these steps measurable. The effect described above is, indeed, restricted to the piles of multilayer in between adjacent antidots (see inset of Fig. 3). The large number of such piles in antidotted samples enhances the contribution to dissipation coming from kinked vortices. The superconductor-air interfaces in samples without antidots, instead, are limited to much smaller zones at the edges, and for low anisotropy the largest contribution to dissipative effects comes from the rigid flux lines present in the bulk of the superconductor.

In conclusion, the critical current density J_c has been measured at different magnetic-field values and orientations in superconducting Nb/CuMn multilayers with different anisotropies both in the absence and presence of an array of antidots. Signatures of the presence of kinked vortices are found in both cases. While in the samples without antidots these effects are limited to highly anisotropic samples, no such limitation is observed for the antidotted case, at least in the appropriate range of field orientations. Moreover, antidotted structures proved to be favorable environments for a direct observation of vortex kink formation, showing low angle modulation of J_c associated to single vortex kinks entering the system.

This work was partially supported by the INFN-ELOISATRON special project.

*Permanent address: State University of Informatics and Radio-Electronics, P. Brovka Str. 6, 220013 Minsk, Belarus.

[†]Also at Dipartimento di Fisica, Università degli Studi di Cagliari, 09042 Monserrato (Ca), Italy.

¹G. Blatter *et al.*, *Rev. Mod. Phys.* **66**, 1125 (1994).

²A.N. Lykov, *Adv. Phys.* **42**, 263 (1993).

³G.W. Crabtree *et al.*, *Proceedings of the NATO Advanced Study Institute on the Physics and Material Science of Vortex States, Flux Pinning and Dynamics*, edited by S. Bose and R. Kosowski (Kluwer Academic Publishers, Kusadasi, Turkey, 1998).

⁴C. Attanasio *et al.*, *Phys. Rev. B* **57**, 6056 (1998).

⁵C. Coccorese *et al.*, *Phys. Rev. B* **57**, 7922 (1998).

⁶A.N. Lykov and Yu.V. Vishnyakov, *Europhys. Lett.* **36**, 625 (1996).

⁷P. Koorevaar *et al.*, *Phys. Rev. B* **49**, 441 (1994).

⁸R. Fastampa *et al.*, *Phys. Rev. Lett.* **67**, 1795 (1991).

⁹P. Koorevaar *et al.*, *Phys. Rev. B* **47**, 934 (1993).

¹⁰S. de Brion *et al.*, *Phys. Rev. B* **49**, 12 030 (1994).

¹¹P.H. Kes *et al.*, *Phys. Rev. Lett.* **64**, 1063 (1990).

¹²A. Barone, A.I. Larkin, and Y.N. Ovchinnikov, *J. Supercond.* **3**, 155 (1990).

¹³M. Tachiki, T. Koyama, and S. Takahashi, *Physica C* **185-189**,

303 (1991).

¹⁴D. Feinberg, *Physica C* **194**, 126 (1992).

¹⁵C. Tom-Rosa *et al.*, *Z. Phys. B: Condens. Matter* **83**, 221 (1991).

¹⁶H. Raffy *et al.*, *Phys. Rev. Lett.* **66**, 2515 (1991).

¹⁷A.T. Fiory, A.F. Hebard, and S. Somekh, *Appl. Phys. Lett.* **32**, 73 (1978).

¹⁸M. Baert *et al.*, *Phys. Rev. Lett.* **74**, 3269 (1995).

¹⁹J.I. Martin *et al.*, *Phys. Rev. Lett.* **79**, 1929 (1997).

²⁰L.V. Mercaldo *et al.*, *Phys. Rev. B* **53**, 14 040 (1996).

²¹C. Attanasio *et al.*, *Phys. Rev. B* **62**, 14 461 (2000).

²²C. Attanasio *et al.*, *Physica C* **312**, 112 (1999).

²³B.Y. Jin and J.B. Ketterson, *Adv. Phys.* **38**, 189 (1989).

²⁴The curve at $\mu_0 H_a = 0.862$ T measured at $T = 3.10$ K behaves differently at high angles, because this field exceeds $H_{c2}(\theta)$ in that angular range.

²⁵L.N. Bulaevskii, M. Ledvij, and V.G. Kogan, *Phys. Rev. B* **46**, 366 (1992).

²⁶A.S. Sidorenko *et al.*, *Fiz. Nizk. Temp.* **6**, 706 (1980) [*Sov. J. Low Temp. Phys.* **6**, 341 (1980)].

²⁷E.H. Brandt, *Phys. Lett.* **77A**, 484 (1980).

²⁸D. Dew-Hughes, *Philos. Mag.* **30**, 293 (1974).